To protect the rights of the author(s) and publisher we inform you that this PDF is an uncorrected proof for internal business use only by the author(s), editor(s), reviewer(s), Elsevier and typesetter TNQ Books and Journals Pvt Ltd. It is not allowed to publish this proof online or in print. This proof copy is the copyright property of the publisher and is confidential until formal publication.

10

c0010 Soft robotics for hand rehabilitation

[AU1] Lizhen Wang[1,2], Guangshuai Peng[1,2], Wei Yao[2,4], Stuart Biggar[2], Yubo Fan[1,2,3]

[1]KEY LABORATORY FOR BIOMECHANICS AND MECHANOBIOLOGY OF MINISTRY OF EDUCATION, SCHOOL OF BIOLOGICAL SCIENCE AND MEDICAL ENGINEERING, BEIHANG UNIVERSITY, BEIJING, CHINA; [2]BEIJING ADVANCED INNOVATION CENTER FOR BIOMEDICAL ENGINEERING, BEIHANG UNIVERSITY, BEIJING, CHINA; [3]NATIONAL RESEARCH CENTER FOR REHABILITATION TECHNICAL AIDS, BEIJING, CHINA; [4]DEPARTMENT OF BIOMEDICAL ENGINEERING, UNIVERSITY OF STRATHCLYDE, GLASGOW, UNITED KINGDOM

Chapter outline

Introduction **1**
Materials and methods **2**
Actuators design and fabrication 2
Actuator characterization 2
Cable drive system 5
User intent detection 6
Results **6**
Conclusions and future trends **7**
References **8**

s0010 Introduction

p0010 About 15 million people are affected by stroke annually around the world [1], and more than 70% of stroke survivors' have damaged hand function to different degrees [2]. The incidence of stroke has been increasing gradually in recent years. The hands play an important role in performing activities of daily living (ADLs) and living an independent life [3]. Physical therapy is an important treatment to improve nerve function for stroke patients; however the current practice is labor intensive, costly, and requires assistance from physical therapists [4].

p0015 Clinical studies indicate that rehabilitation robots give significant improvement in functional gains under intense therapy [5]. There are a number of rehabilitation devices have been developed in this field [6,7]. Currently, the majority of hand rehabilitation and assistive devices consist of multi-degree of freedom linkage structures [8–11], however

Intelligent Biomechatronics in Neurorehabilitation. https://doi.org/10.1016/B978-0-12-814942-3.00010-6

Copyright © 2020 Elsevier Inc. All rights reserved.

10010-HU-9780128149423

These proofs may contain color figures. Those figures may print black and white in the final printed book if a color print product has not been planned. The color figures will appear in color in all electronic versions of this book.

To protect the rights of the author(s) and publisher we inform you that this PDF is an uncorrected proof for internal business use only by the author(s), editor(s), reviewer(s), Elsevier and typesetter TNQ Books and Journals Pvt Ltd. It is not allowed to publish this proof online or in print. This proof copy is the copyright property of the publisher and is confidential until formal publication.

these rigid exoskeleton robots are bulky, heavy, costly, and inaccessible outside of a clinical setting [2].

p0020 Panagiotis Polygerinos summarized the design requirements of wearable hand rehabilitation devices [12], where the weight of the device mounted on the hand should be less than 0.5 kg. The power, control, and actuators of a device can be mounted on the waist or back, and the weight should not exceed 3 kg. The device also needs to be customizable to the user's hand size. In addition, in order to not resist the motion of the fingers when the device is not powered, the device should be made from soft and compliant material [13].

p0025 Rigid exoskeletons are not the only solution that can be used for hand rehabilitation. More recently, a list of hand rehabilitation devices combined with soft and compliance materials such as tendon drive or fluidic soft actuators for hand rehabilitation have appeared and been used in hand rehabilitation [14–19]. These devices can provide assistance with ADLs and hand rehabilitation without rigid joints and links. These soft hand rehabilitation robots are more compact, lightweight, accessible, and easy to don and doff.

p0030 In this chapter, we introduce a new soft and wearable robotic glove which is based on a cable drive system and pneumatic artificial muscles. The main goal of this design is to develop a soft robotic glove that is both lightweight and low cost.

s0015 Materials and methods

s0020 Actuators design and fabrication

p0035 The McKibben pneumatic artificial muscle (PAM) was developed in the 1950s by physician Joseph L. McKibben for actuating orthotics [20,21]. McKibben PAMs have been used for many years due to their unique set of capabilities and features including low cost and high power-to-weight ratio. A typical McKibben PAM consists of an inflatable inner tube, an external braided mesh, and pneumatic fitting. On the basis of previous research achievements [22], the composition material of the PAM used in this chapter is presented in Fig. 10.1A, including a balloon acting as the inner tube, an external braided mesh with Nylon material, and a segment of PU tube used as a pneumatic fitting. Once the inner tube is pressurized, the external braided mesh contracts axially and dilates radially (Fig. 10.1B).

s0025 Actuator characterization

p0040 Using the theory of energy conservation, the force produced by a PAM can be described as:

$$F = -p\frac{dV}{dl} \tag{10.1}$$

where F is output force, p is internal air pressure, V is the PAM volume, and l is the PAM length. The relevant parameters are defined in Fig. 10.2.

These proofs may contain color figures. Those figures may print black and white in the final printed book if a color print product has not been planned. The color figures will appear in color in all electronic versions of this book.

To protect the rights of the author(s) and publisher we inform you that this PDF is an uncorrected proof for internal business use only by the author(s), editor(s), reviewer(s), Elsevier and typesetter TNQ Books and Journals Pvt Ltd. It is not allowed to publish this proof online or in print. This proof copy is the copyright property of the publisher and is confidential until formal publication.

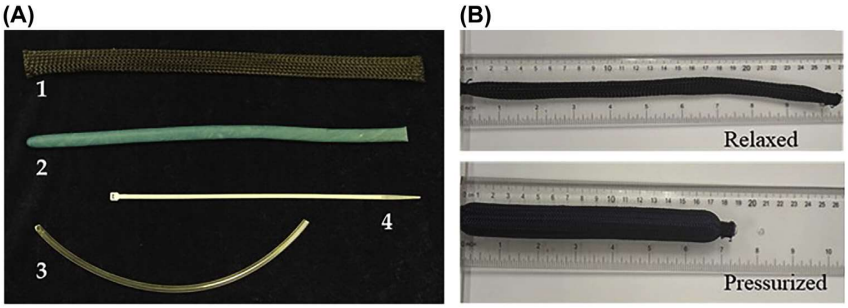

f0010 **FIGURE 10.1** Design and fabrication of a PAM: (A) The composition material of a PAM: (1) braided mesh, (2) inflatable inner tube, (3) a segment of PU tube, (4) zip tie. (B) An assembled PAM.

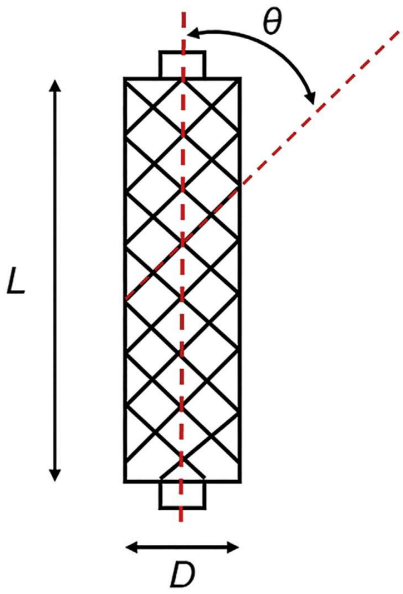

f0015 **FIGURE 10.2** Illustration of parameters.

p0045 Supposing that there is zero wall thickness and zero friction between the mesh and tube, the force output can be derived:

$$F = p\frac{\pi D_0^2}{4}\left(3\cos^2\theta - 1\right) \tag{10.2}$$

where θ is the braid angle, and D_0 is the diameter of the mesh when θ equal to 90 degrees. The force output is linearly proportional to the pressure and the PAM length. The force

These proofs may contain color figures. Those figures may print black and white in the final printed book if a color print product has not been planned. The color figures will appear in color in all electronic versions of this book.

To protect the rights of the author(s) and publisher we inform you that this PDF is an uncorrected proof for internal business use only by the author(s), editor(s), reviewer(s), Elsevier and typesetter TNQ Books and Journals Pvt Ltd. It is not allowed to publish this proof online or in print. This proof copy is the copyright property of the publisher and is confidential until formal publication.

output of a PAM is determined by its inner air pressure and its contraction, as shown in Eq. (10.2) [23].

p0050 An isometric contraction test and constant pressure contraction test were used to evaluate PAMs [24]. Both tests are carried out using a tensile testing machine (Figs. 10.3A and 10.4A). The force–pressure curve (Fig. 10.3B) shows that the artificial muscle could generate force reaching 100 N in a constant pressure 180 kPa, which should be enough to meet the requirements of 6–10 N in the fingertip for ADLs [22]. The force–contraction curve (Fig. 10.4B) shows that the percent contraction is up to 32% at a pressure of 200 kPa.

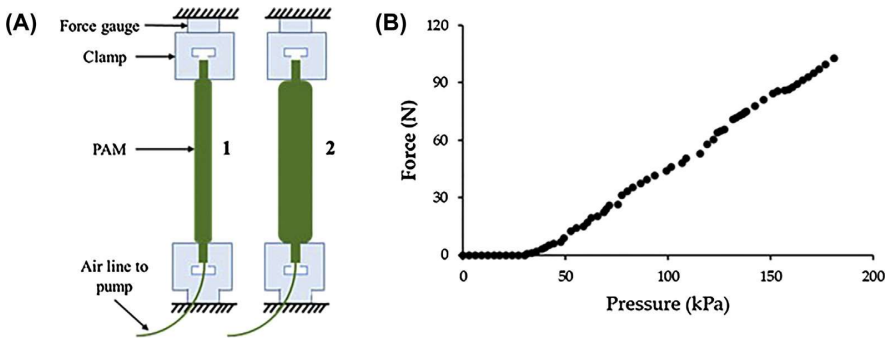

f0020 **FIGURE 10.3** Isometric contraction test: (A) the schematic of the test procedure; (B) the force–pressure curve.

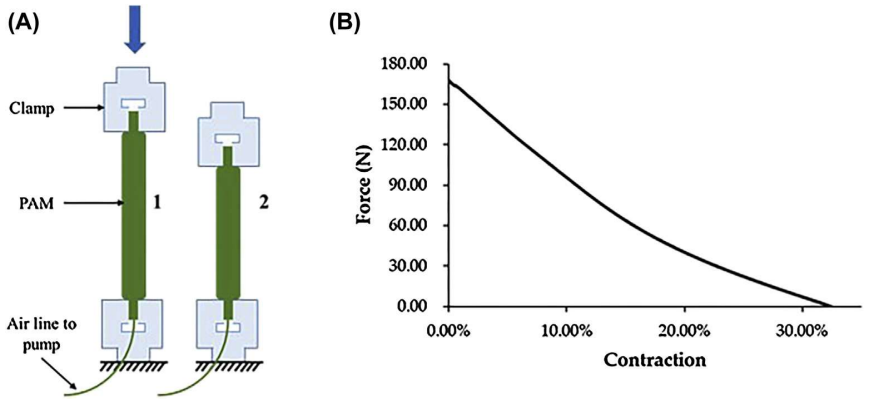

f0025 **FIGURE 10.4** Constant pressure contraction test: (A) the schematic of the test procedure; (B) the force–contraction curve.

These proofs may contain color figures. Those figures may print black and white in the final printed book if a color print product has not been planned. The color figures will appear in color in all electronic versions of this book.

To protect the rights of the author(s) and publisher we inform you that this PDF is an uncorrected proof for internal business use only by the author(s), editor(s), reviewer(s), Elsevier and typesetter TNQ Books and Journals Pvt Ltd. It is not allowed to publish this proof online or in print. This proof copy is the copyright property of the publisher and is confidential until formal publication.

s0030 Cable drive system

p0055 In order to reduce the weight of this robotic glove, the user's own skeleton is used to transfer force and torque. The whole structure of the cable drive system consisted of a soft glove, cable guides, cables, and PAMs. The PAMs are mounted on the forearm in order to reduce the weight applied to the hand (Fig. 10.5). The total weight of the glove part is about 120 g. The glove part is sufficiently light for stroke patients. Additionally, as the PAMs are worked under air pressure, thus they do not distribute extra weight to the forearm when the actuators are pressurized. The ring finger and little finger were not motorized as they do not play a key role in the grasp motion [4].

p0060 An electro-pneumatic control system was developed to allow isolated control of each PAM. The electro-pneumatic control system consisted of a microcontroller (stm32f103zet6, Telesk, China), air pressure sensors (XGZP6847, Risym, China), and miniature solenoid valves (T101U-F, Ousituo, China). Pressure sensors were used to monitor the internal pressure of the PAMs. The controller uses pulse width modulation (PWM) to control the working condition of the valves and pump according to the internal pressure of the PAMs (Fig. 10.6).

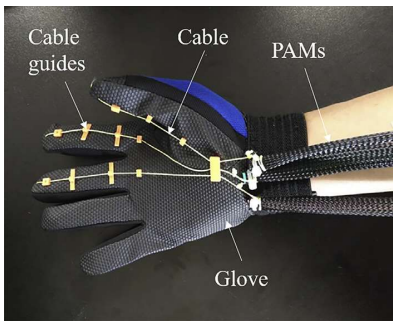

f0030 **FIGURE 10.5** The cable drive system based on PAMs.

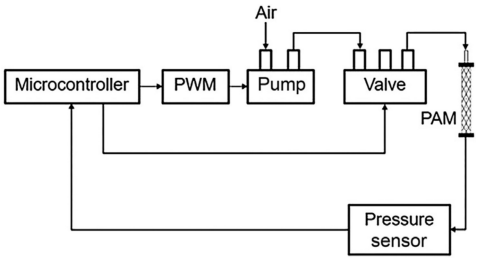

f0035 **FIGURE 10.6** The electro-pneumatic control system of the robotic glove.

These proofs may contain color figures. Those figures may print black and white in the final printed book if a color print product has not been planned. The color figures will appear in color in all electronic versions of this book.

To protect the rights of the author(s) and publisher we inform you that this PDF is an uncorrected proof for internal business use only by the author(s), editor(s), reviewer(s), Elsevier and typesetter TNQ Books and Journals Pvt Ltd. It is not allowed to publish this proof online or in print. This proof copy is the copyright property of the publisher and is confidential until formal publication.

s0035 User intent detection

p0065 User intent of bending and extending fingers can be detected by measuring the sEMG of muscles on the forearm. In this work, we used the healthy hand to control the activities of the robotic glove on the affected hand, where the electrical impulses of the muscle can be used to directly control finger movements. This strategy is suitable for stroke patients with hemiplegia.

p0070 In order to measure the activities of the muscles of the forearm, two sEMG sensors were placed on the forearm. The first sEMG sensor was placed at the flexor digitorum superficialis (FDS), which mainly flexes the fingers. The second sEMG sensor was placed at the extensor digitorum communis (EDC), which mainly extends the fingers. Therefore, sEMG was obtained in two signals. The signals were sent to the microcontroller. A new open-loop sEMG logic proposed by Panagiotis Polygerinos et al. [3] has been adopt to judge the user intent. The control of the soft robotic glove can be realized by continuously monitoring the state of the two muscle signals (FDS and EDC) to three predefined conditions: (a) "flex," (b) "extend," and (c) "hold" [25]. The flex condition can be achieved when the sEMG acquired from the FDS muscles is over the flexor threshold, while at the same time, the sEMG acquired from the EDC muscles is below the extensor threshold. In this condition, the PAMs will be pressurized and drive the fingers in flexion. The extend condition will be achieved when the sEMG acquired from the FDS muscles is below the flexor threshold, while at the same time, the sEMG acquired from the EDC muscles exceeds the extensor threshold. In this condition, the PAMs will be depressurized and open the hand. The hold condition can be achieved when neither the flex nor extend conditions are meet. The PAMs inner air pressure will stay unchanged in this condition. The threshold depends on a number of factors and it is different from person to person. The threshold can be adjusted according to the power of the user's sEMG signal.

s0040 Results

p0075 We experimentally investigated the performance of the robotic glove by testing the device with one healthy 25-year-old male subject. An air pressure regulator and a force sensor were used to test the force applied by the index finger tip. We measured the force of the healthy male subject's index finger tip while wearing the robotic glove (Fig. 10.7). When the PAM was pressurized, the fingertip applied a vertical force on the force sensor.

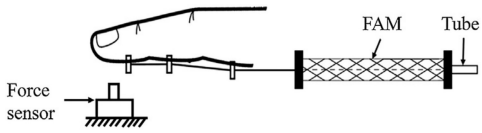

f0040 **FIGURE 10.7** The platform for the finger tip force test.

These proofs may contain color figures. Those figures may print black and white in the final printed book if a color print product has not been planned. The color figures will appear in color in all electronic versions of this book.

To protect the rights of the author(s) and publisher we inform you that this PDF is an uncorrected proof for internal business use only by the author(s), editor(s), reviewer(s), Elsevier and typesetter TNQ Books and Journals Pvt Ltd. It is not allowed to publish this proof online or in print. This proof copy is the copyright property of the publisher and is confidential until formal publication.

t0010 **Table 10.1** The ROM of finger joints when wearing the robotic glove.

Index finger joint	The range of motion in active motion	The range of motion in passive motion
MCP	63.25 degrees	58.02 degrees
PIP	79.12 degrees	57.36 degrees
DIP	45.32 degrees	40.13 degrees

The maximum fingertip force measured was up to 12 N when the pressure of the PAM was 180 kPa, which is sufficient for performing activities of daily living.

p0080 To evaluate the kinematic performance of the soft robotic glove, high-speed cameras were used to film finger motion of the healthy subject while he was wearing the robotic glove. The range of motion (ROM) of index finger joints is shown in Table 10.1, sufficient ROM of the index finger was achieved with the assistance of this device. Although the range of the ROM was smaller than that of voluntary movement when the subject was not wearing the device, it was enough to perform pinch and wrap grasp activities.

p0085 With the help of this device, a healthy subject grasped the following target objects: (a) a cube, (b) a plastic bottle containing 300 mL of water, (c) an apple, (d) a smart phone, (e) a pen, and (f) a mouse, to test the ability of the robotic glove to provide assistance in activities of daily living. The subject successfully grasped all the objects for the first time using the robotic glove due to the simple control scheme and good adaption mechanism (Fig. 10.8).

s0045 Conclusions and future trends

p0090 In this chapter, a new soft and wearable robotic glove that uses a tendon drive system and PAMs was designed. The weight of the glove part is about 120 g. The weight of the control box, which contains a battery, pump, and microcontroller, is about 2 kg. The robotic glove is compact and lightweight, making it more accessible than rigid hand exoskeleton robots. The myoelectric control strategy was used to control the robotic glove. A new open-loop sEMG logic has been adopted to judge user intent. The maximum fingertip force is about 12 N, which should be enough to provide assistance in ADLs. Finally, with the help of the device subjects were capable of grasping objects of various shapes. The soft and wearable robotic glove can meet the requirements for stroke rehabilitation.

p0095 There are some limitations to the cable drive system. The cables fixed between finger tips and PAMs could restrict movement of the wrist and cause injury. In the future, steps to improve the performance and safety of the cable drive system and to develop a more intelligent human–robot interface to detect user intent such as brain-computer interface will be targeted. Also, stroke subjects will be involved in testing in the future.

These proofs may contain color figures. Those figures may print black and white in the final printed book if a color print product has not been planned. The color figures will appear in color in all electronic versions of this book.

To protect the rights of the author(s) and publisher we inform you that this PDF is an uncorrected proof for internal business use only by the author(s), editor(s), reviewer(s), Elsevier and typesetter TNQ Books and Journals Pvt Ltd. It is not allowed to publish this proof online or in print. This proof copy is the copyright property of the publisher and is confidential until formal publication.

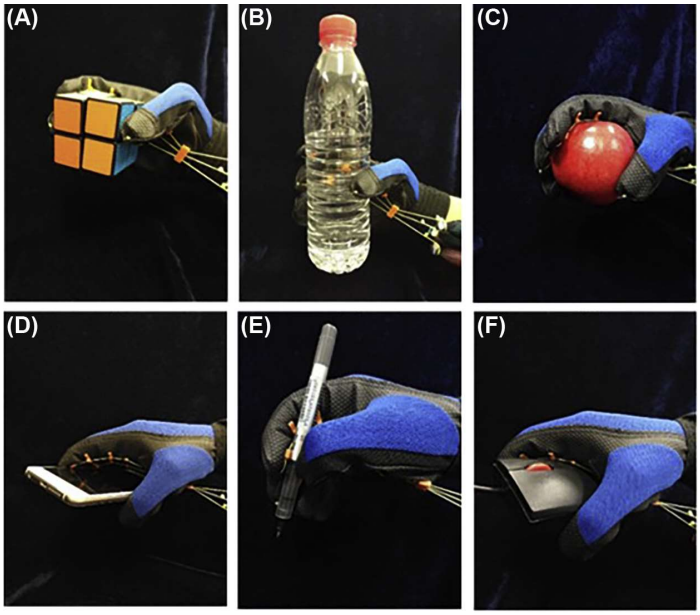

f0045 **FIGURE 10.8** Using the robotic glove to pinch and grasp various objects: (A) a cube; (B) a plastic bottle containing 300 mL of water; (C) an apple; (D) a smart phone; (E) a pen; and (F) a mouse.

p0100 Soft robots have the advantages of light weight, continuous deformation, and strong adaptability, providing a new way to break through the limitations of traditional rigid robots. Soft robots have broad application prospects in military, medical, and industrial fields.

References

[1] Takahashi CD, Der-Yeghiaian L, Le V, Motiwala RR, Cramer SC. Robot-based hand motor therapy after stroke. Brain 2008;131:425–37.

[2] Schabowsky CN, Godfrey SB, Holley RJ, Lum PS. Development and pilot testing of hexorr: hand exoskeleton rehabilitation robot. Journal of NeuroEngineering and Rehabilitation 2010;7:36.

[3] Polygerinos P, Galloway KC, Sanan S, Herman M, Walsh CJ. EMG controlled soft robotic glove for assistance during activities of daily living. In: 2015 IEEE international conference on rehabilitation robotics (ICORR). IEEE; 2015.

[4] Biggar S, Yao W. Design and evaluation of a soft and wearable robotic glove for hand rehabilitation. EEE Transactions on Neural Systems and Rehabilitation Engineering 2016;24:1071–80.

[5] Wolf SL, Winstein CJ, Miller JP, Taub E, Uswatte G, Morris D, et al. Effect of constraint-induced movement therapy on upper extremity function 3 to 9 months after stroke: the excite randomized clinical trial. The Journal of the American Medical Association 2006;296:2095–104.

These proofs may contain color figures. Those figures may print black and white in the final printed book if a color print product has not been planned. The color figures will appear in color in all electronic versions of this book.

To protect the rights of the author(s) and publisher we inform you that this PDF is an uncorrected proof for internal business use only by the author(s), editor(s), reviewer(s), Elsevier and typesetter TNQ Books and Journals Pvt Ltd. It is not allowed to publish this proof online or in print. This proof copy is the copyright property of the publisher and is confidential until formal publication.

[6] Nef T, Riener R. ARMin - design of a novel arm rehabilitation robot. In: 2005 IEEE international conference on rehabilitation robotics (ICORR). IEEE; 2005. p. 57–60.

[7] Loureiro R, Amirabdollahian F, Topping M, Driessen B, Harwin W. Upper limb robot mediated stroke therapy – GENTLE/s approach. Autonomous Robots 2003;15:35–51.

[8] Heo P, Gwang MG, Lee SJ, Rhee K, Kim J. Current hand exoskeleton technologies for rehabilitation and assistive engineering. International Journal of Precision Engineering and Manufacturing 2012; 13:807–24.

[9] Jones CL, Wang F, Morrison R, Sarkar N, Kamper DG. Design and development of the cable actuated finger exoskeleton for hand rehabilitation following stroke. IEEE 2014;19:131–40.

[10] Lee SW, Landers KA, Park HS. Development of a biomimetic hand exotendon device (biomHED) for restoration of functional hand movement post-stroke. IEEE Transactions on Neural Systems and Rehabilitation Engineering 2014;22:886–98.

[11] Dicicco M, Lucas L, Matsuoka Y. Comparison of control strategies for an EMG controlled orthotic exoskeleton for the hand. In: 2004 IEEE international conference on robotics and automation (ICRA). IEEE; 2004. p. 1622–7.

[12] Panagiotis P, Wang Z, Galloway KC, Wood RJ, Walsh CJ. Soft robotic glove for combined assistance and at-home rehabilitation. Robotics and Autonomous Systems 2014;73:135–43.

[13] Aubin PM, Sallum H, Walsh C, Stirling L, Correia A. A pediatric robotic thumb exoskeleton for at-home rehabilitation: the Isolated Orthosis for Thumb Actuation (IOTA). In: 2013 IEEE 13th international conference on rehabilitation robotics (ICORR). IEEE; 2013.

[14] Radder B, Kottink A, Vaart NVD, Oosting D, Buurke JH, Nijenhuis SM. User-centred input for a wearable soft-robotic glove supporting hand function in daily life. In: 2015 IEEE international conference on rehabilitation robotics (ICORR). IEEE; 2015. p. 502–7.

[15] Zhao HC, Huang RK, Shepherd RF. Curvature control of soft orthotics via low cost solid-state optics. In: 2016 IEEE international conference on robotics and automation (ICRA). IEEE; 2016. p. 4008–13.

[16] Zhao H, Jalving J, Huang R, Knepper R, Ruina A, Shepherd R. A helping hand: soft orthosis with integrated optical strain sensors and EMG control. IEEE Robotics and Automation Magazine 2016; 23:55–64.

[17] In H, Kang BB, Sin MK, Cho KJ. Exo-glove: a wearable robot for the hand with a soft tendon routing system. IEEE Robotics and Automation Magazine 2015;22:97–105.

[18] Nycz CJ, Delph MA, Fischer GS. Modeling and design of a tendon actuated soft robotic exoskeleton for hemiparetic upper limb rehabilitation. In: International conference of the IEEE engineering in medicine and biology society (EMBC). IEEE; 2015. p. 3889–92.

[19] Park S, Bishop L, Post T, Xiao Y, Stein J, Ciocarlie M. On the feasibility of wearable exotendon networks for whole-hand movement patterns in stroke patients. In: 2016 IEEE international conference on robotics and automation (ICRA). IEEE; 2016. p. 3729–35.

[20] Tondu B. Modelling of the mckibben artificial muscle: a review. Journal of Intelligent Material Systems and Structures 2012;23:225–53.

[21] Tondu B, Lopez P. Modeling and control of McKibben artificial muscle robot actuators. IEEE Control Systems Magazine 2000;20:15–38.

[22] Yi J, Shen Z, Song C, Wang Z. A soft robotic glove for hand motion assistance. In: 2016 IEEE international conference on real-time computing and robotics (RCAR). IEEE; 2016. p. 111–6.

[23] Tian Y, Wang K, Yi J, Wang Z, Chen MZQ. Introduction to modeling of the McKibben pneumatic artificial muscle with end constraints. In: 2016 IEEE international conference on information and automation. IEEE; 2016. p. 1624–9.

These proofs may contain color figures. Those figures may print black and white in the final printed book if a color print product has not been planned. The color figures will appear in color in all electronic versions of this book.

To protect the rights of the author(s) and publisher we inform you that this PDF is an uncorrected proof for internal business use only by the author(s), editor(s), reviewer(s), Elsevier and typesetter TNQ Books and Journals Pvt Ltd. It is not allowed to publish this proof online or in print. This proof copy is the copyright property of the publisher and is confidential until formal publication.

[24] Obiajulu SC, Roche ET, Pigula FA, Walsh CJ. Soft pneumatic artificial muscles with low threshold pressures for a cardiac compression device. In: ASME international design engineering technical conferences/computers and information in engineering conference (IDETC/CIE). ASME; 2013. p. 1–8.

[25] Hong KY, Ang BWK, Lim JH, Goh JCH, Yeow CH. A fabric-regulated soft robotic glove with user intent detection using EMG and RFID for hand assistive application. In: Proceeding of the IEEE international conference on robotics and automation (ICRA), Stockholm, Sweden, 16–21 May, 2016; 2016. p. 3537–42.

These proofs may contain color figures. Those figures may print black and white in the final printed book if a color print product has not been planned. The color figures will appear in color in all electronic versions of this book.